# GRAVITATIONAL LENSING -- MODELS

Ramesh Narayan
Steward Observatory
University of Arizona
Tucson, AZ 85721, U.S.A.

ABSTRACT. Qualitative features of gravitational lensing are discussed in terms of a scalar framework based on Fermat's principle. The lensing action of galaxy-like models with spherical and elliptical mass distributions are described. The elliptical model has three distinct regimes of lensing, of which two correspond to lensing with three images and one with five images. One of the three-image geometries has been frequently explored in the past. Models proposed for 0957+561 correspond to this. The five-image geometry has been invoked for 1115+080. Some general model-independent properties of gravitational lensing are listed. If image parities were available, it might be possible to make statements about the lensing mass even when it is made up of dark matter.

## 1. INTRODUCTION

Presently, seven probable cases of gravitational lensing of a high redshift quasar by foreground matter have been identified (see Burke, this volume, for a review of the observations). Attempts to model some of these are briefly reviewed here. A feature to note is that some of the observed cases of lensing (e.g. 0957+561, 2016+112) provide fairly strong constraints on models through a variety of observational details, while in other cases (e.g. 2345+007, 1635+267) the only available information is the angular separation and relative magnifications of the two images. In particular, no trace of the lensing matter is seen in these latter cases. In the light of this wide range of modeling requirements, only a qualitative discussion of lens models will be attempted here. Different regimes of lensing by a galaxy-like elliptical (in projection) lens distribution will be identified and the various known cases of lensing will be discussed within this framework.

Gravitational lensing is usually discussed in terms of a vector formalism (Bourassa and Kantowski 1975, Young et al. 1980) where the position of an image in the sky and that of the undeflected source are related through the vector deflection produced by the lens. This relationship is usually picturised through a bending angle diagram (e.g. Young et al. 1980), but this is possible only when the lensing distribution is circularly symmetric in projection in which case all the vectors in the problem are

529

·parallel to one another. For the elliptical lenses that we are interested in here, it is more convenient to consider a scalar formalism in terms of Fermat's principle (Nityananda 1986, Schneider 1985, Blandford, Narayan and Nityananda 1986, BNN).

## 2. THE TIME SURFACE AND FERMAT'S PRINCIPLE

Consider a source at redshift $z_S$ being gravitationally lensed by matter distributed in a thin slab at redshift $z_L$. Let $\theta_S$ be the angular position in the sky of the source in the absence of the lens. In the presence of the lens, we can define a time-delay surface as follows. Consider a ray that propagates along a null geodesic from the source to the lens plane and then along another null geodesic from there to the observer so as to arrive along the angular direction $\theta_I$. The time delay along this virtual ray path, relative to the direct ray from the source to the observer in the absence of the lens, is given by

$$
\begin{aligned}
t(\theta_I) &= t_{geom}(\theta_I) + t_{grav}(\theta_I) \\
&= \frac{(1+z_L)d_{OS}d_{OL}}{2cd_{LS}}(\theta_I - \theta_S)^2 - \frac{2(1+z_L)}{c^3}\int \phi(\theta_I d_{OL}, s)ds
\end{aligned}
\tag{1}
$$

The geometrical time-delay $t_{geom}$ due to the extra path-length takes the form of a paraboloid with its minimum at $\theta_I = \theta_S$. The $d$'s are angular diameter distances between the observer, lens and source. The gravitational time-delay $t_{grav}$ arises because light travels slower in the presence of gravitating matter and is proportional to the integral along the ray of the Newtonian potential $\phi$. Thus, the surface $t(\theta_I)$ corresponding to the total time-delay is obtained by taking the paraboloidal surface $t_{geom}$ and pushing it up by an amount proportional to the depth of the two-dimensional potential of the projected lens. This time-delay surface has the following properties (BNN):

(a) By Fermat's Principle, true images are located at those $\theta_I$ which correspond to extrema in the time-surface. Three types of extrema are possible -- Lows (represented by the symbol L), Highs (H) and Saddle-points (S).

(b) The relative time-delay between two images is directly given by the height difference in the time-surface at the two extrema. Time-delays can be measured if the source is variable.

(c) At a given extremum, the time-surface can be locally described by a curvature tensor $\partial^2 t/\partial\theta_{I1}\partial\theta_{I2}$. If $\lambda_1$ and $\lambda_2$ are the principal curvatures, then the magnification of the image is proportional to $|\lambda_1\lambda_2|^{-1}$. The relative magnifications of different images are directly observable.

(d) The partial parities of the image along the principal axes are given by the signs of $\lambda_1$ and $\lambda_2$ respectively (L and H correspond to $+ +$ and $- -$ and S to $+ -$ or $- +$, see Figure 1). The total parity is given by the sign of $\lambda_1\lambda_2$ ($+$ for L and H and $-$ for S). Relative parities between different images can be observed if the source has resolved VLBI structure (e.g. a bent jet) or an asymmetric optical fuzz.

In the absence of the lens, the time-surface has a single extremum of type L at $\theta_I = \theta_S$. When the surface is distorted by the presence of lensing
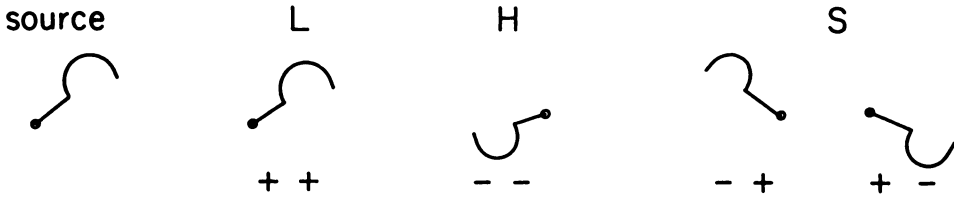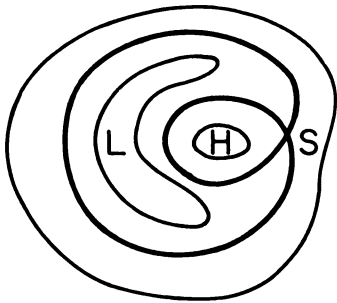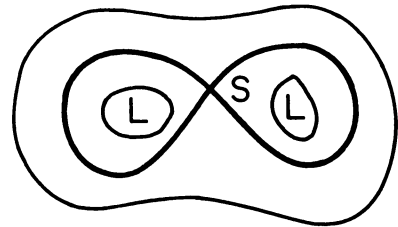
source            L            H                    S

+ +          – –            – +        + –

Figure 1.  Partial parities associated with different types of extrema

(a) limacon                              (b) lemniscate

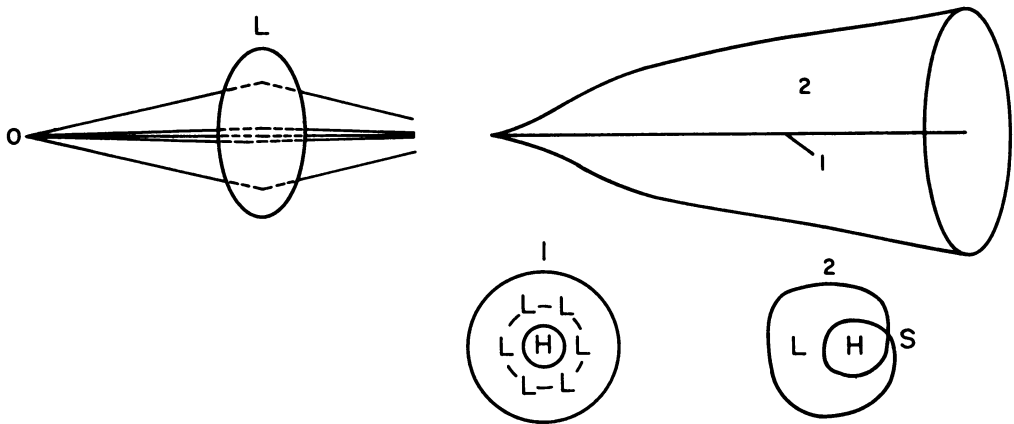Figure 2.  Time-delay contours for the two possible three-image topologies

Figure 3.  Lensing by a circularly symmetric lens

matter, new images can be produced, but invariably in pairs so that there is always an odd number of images (Burke 1981). There are only two topological arrangements of extrema possible with three images, as shown by the contours of time-delay in Figure 2 (BNN). These topologies are completely defined by drawing the contour that passes through the S image (thick lines in Figure 2). This is the only contour that is not topologically equivalent to a circle and the two possibilities are called the 'limacon' and 'lemniscate' respectively. With five images, there are two S images and hence two non-simple contours. This leads to six possible topologies (BNN).

## 3. CIRCULARLY SYMMETRIC LENS

We begin with this simple case and consider in Figure 3 the three-dimensional source space behind a typical circularly-symmetric galaxy-like lens with a non-singular core. The conical surface on the right of the figure separates source positions outside it, where only one image is seen by the observer at O, from positions inside it corresponding to three images. This surface is a caustic sheet since a point source located on this sheet leads to one normal image and a pair of infinitely magnified merging images. In terms of catastrophe theory (Poston and Stewart 1978), the sheet corresponds to a 'fold' catastrophe. For source positions along the axis of cylindrical symmetry, the observer sees one image at the lens center and an infinitely magnified circular ring around it. The time-surface in this case takes the shape of a Mexican hat, with the central image at H in the center and the ring image at the bottom of the surrounding trough. For off-center positions of the source (within the conical fold sheet), the time-surface takes the form of a tilted Mexican hat and so the three images correspond to the limacon topology of Figure 2a.

## 4. ASTIGMATIC LENS

The ring-image geometry obtained with the circular lens is very special and is destroyed in the presence of any perturbation in the shape of the lens or in the isotropy of the background. Another way of seeing this is to note that there is no generic catastrophe that corresponds to the infinite magnification obtained with this geometry. Because of this non-genericity, studies of high amplification events in gravitational lensing should avoid the circularly symmetric lens, though this is not widely recognised.

A simple way to make the circular lens generic is to introduce some astigmatism so that the focusing power of the lens along its two principal axes are not equal. Figure 4 shows the situation in this case for a typical galaxy-like potential (BNN). In the 'far-field' region of source space (i.e. for a source located far beyond the lens), the ring-image line of Figure 3 'unfolds' into a region corresponding to five images with the characteristic topology marked 3 in Figure 4. This topology is most easily visualized as a squeezed Mexican hat where the bottom of the trough, instead of having a constant height, develops two minima and two maxima along its circumference. The five-image and surrounding three-image regions

(marked 2) are separated by a new caustic sheet which consists of four fold sheets connected at four 'cusp' lines. The situation in the 'near-field' region of source space is equally interesting. The single cone of Figure 3 now splits into two sheets that form at the points A and B, corresponding to the different focusing powers along the principal axes of the lens. The region between these two sheets (region 1 in Figure 4) gives the lemniscate three-image topology (Figure 2b), which characteristically forms when the lens is able to split images only along one principal axis and not the other. The two sheets (with two cusp lines each) penetrate each other in an interesting way, forming two 'hyperbolic umbilic' catastrophes at the points marked U.

Thus the average non-singular astigmatic lens produces both possible three-image toplogies and one of six possible five-image topologies. Models of the known cases of gravitational lensing have usually involved elliptic lenses of some sort and therefore correspond to one of the three topologies of Figure 4.
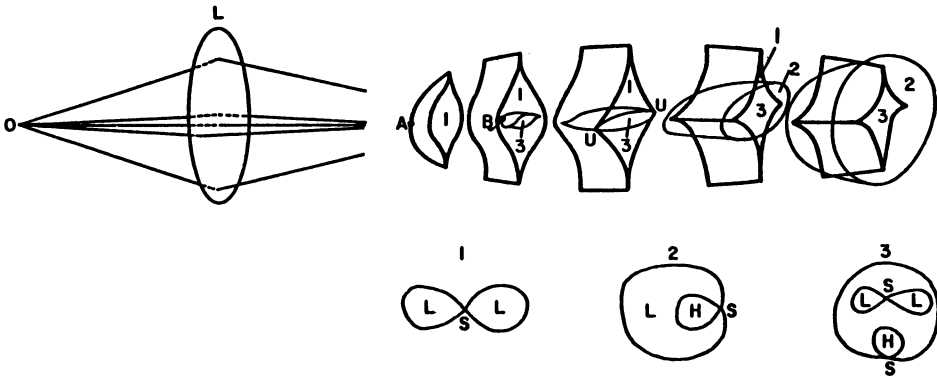
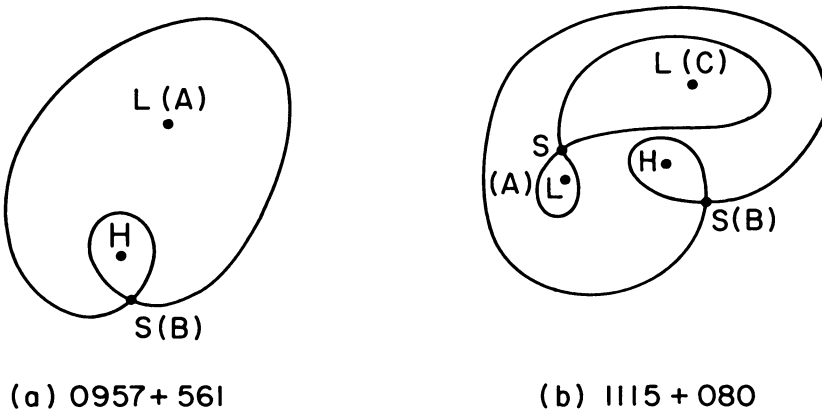Figure 4. Lensing by an astigmatic lens

(a) 0957 + 561                          (b) 1115 + 080

Figure 5. Qualitative features of models of 0957+561 and 1115+080

## MODELS OF LENSES

### 0957+561

Extensive observational data, including VLBI information on parities, are available on 0957+561 and this is consequently the most widely modeled among the known cases of gravitational lensing (Young *et al.* 1981b, Greenfield 1981, Narasimha *et al.* 1984). All the models are similar in their qualitative features, shown in Figure 5a. The topology is that of the limacon, with the A and B images located on L and S respectively. The core of the lensing galaxy produces a third image at H. The galaxy has been detected, but not the image H. The models explain the absence of H by using a small enough core radius for the lensing galaxy, thus making this image very weak. The parity of B is reversed with respect to A. However, the negative parity axis is perpendicular to the line SH, and the VLBI jet points almost exactly along SH (Porcas *et al.* 1981), making it difficult to confirm the reversed parity. More recent observations have apparently succeeded in determining the parities of the images (Burke, private communication, this meeting). It is obvious from Figure 5a that A has a smaller time-delay than B and so it will vary first. Observations seem to confirm this (Florentin-Nielsen 1984). The observed galaxy lens in 0957+561 is not massive enough to produce the 6″ image splitting. Therefore all models invoke the additional effect of a surrounding cluster. This has the effect of introducing extra convergence and shear in the rays from the quasar, but does not affect any of the qualitative features described above.

Most other examples of two-image lensing are probably similar to 0957+561 in their qualitative features. The model of 2345+007 by Subramanian and Chitre (1984) is novel in that it uses two galaxies at different redshifts, but may still have a topology similar to Figure 5a. 2016+112 is a particularly difficult case to model since there are three primary images forming a triangle with angles ~ 90°, 60°, 30°, two additional blobs which may or may not be images, and two possible lensing galaxies (Schneider *et al.* 1986). No model has been proposed so far that fits all the data.

### 1115+080

Models that have been proposed for 1115+080 (Young *et al.* 1981a, Narasimha *et al.* 1982) use a non-spherical galaxy-like lens in the far-field five-image region (marked 3) of Figure 4. The topology is shown in Figure 5b. The source is assumed to be close to the caustic sheet separating the five- and three-image regions and so two of the five images are close together and magnified. The split A image (distinguished individually as $A_1$, $A_2$) is identified with this pair. The B and C images are located on S and L. (The identification of these two images could be reversed since there is a fair degree of symmetry between them.) The missing fifth image is again on H in the core of the lens, somewhere in the middle of the circle formed by the other four images. The fact that no lensing galaxy is seen has been somewhat embarrassing for the models. Nityananda (1986) presents an elegant analysis of this model of 1115+080, showing that the magnifica-

tions $M$ of the four images satisfy $M(A_1) \sim M(A_2)$, $M(B) \sim M(C)$ and $M(A_1)/M(B) \sim AB/A_1A_2$ (ratio of angular separations). As regards time-delays, the image C on L (Figure 5b) is the first to vary, the merging pair A varies next, and the image B on S varies last. The time-delay between $A_1$ and $A_2$ is very small compared to the other delays.

## Lemniscate Models

Models using the lemniscate topology of Figure 2b have rarely been used since they usually require that the lens should under-focus along one of its principal axes, which is unlikely with galaxy lenses that are located 'half-way' to a source at a cosmological distance. Applications include lensing by a supercluster filament (Sanders *et al.* 1984), and lensing by a straight cosmic string (Vilenkin 1984, Hogan and Narayan 1984, Gott 1984), where the missing image is on the string at S. It is tempting to speculate that 2237+031 corresponds to the lemniscate topology since the lensing galaxy is at such a low redshift that it could well under-focus along one axis. In this connection it is important to note that the lemniscate topology can be observationally distinguished from the limacon topology of 0957+561 through image parities.

## 6. SOME 'THEOREMS' IN GRAVITATIONAL LENSING

There is considerable evidence to suggest that dark matter plays an important role in the observed gravitational lenses. Firstly, in several of the cases there is no visible sign of the lensing matter. Secondly, in both 0957+561 and 2016+112, the two cases with the most information on images and 'lensing' galaxies, there is no successful model where the lensing mass follows the light. Once one concedes the presence of dark matter there is a great deal of freedom in modeling, and it is not clear whether it is worthwhile making very detailed models. An alternative approach is to make general inferences about a particular lens that are model-independent. Some possibly useful 'theorems' (BNN) in this regard are listed below:

(a) In general there are an odd number, $2n+1$, of images, of which $n$ are of type S and $n+1$ are of type L or H, with at least one L among these.

(b) The first image to vary is always of type L and therefore has positive (i.e. majority) parity. If this is violated by observations, then one can conclude that some images have gone undetected.

(c) Because mass is positive, all L images are magnified compared to the unlensed source.

(d) A critical surface density $\Sigma_c$ can be defined which is the density a sheet placed at the lens plane should have in order to barely focus rays from the source at the observer. It can be shown that rays corresponding to images of type H and L pass through regions of the lens plane with $\Sigma > \Sigma_c$ and $\Sigma < \Sigma_c$ respectively. Nothing can be said about type S images.

(e) Because topologies such as the lemniscate of Figure 2b with no H images are possible, it is possible to obtain multiple images even with $\Sigma < \Sigma_c$ throughout the lens plane.

(f) Images can be infinitely demagnified when they form on singulari-ties in the lens. This can happen only to H and S images, not to L. We con-clude the following for three-image topologies: (i) If the missing image is lost on a point singularity such as a black hole, then it is of type H and so the remaining images should have opposite parities (Figure 2a); (ii) If on a line singularity such as a cosmic string, then it is likely to be type S and so the other two images will have the same parity (Figure 2b).

(g) In general, the more magnified the images are (small curvature of the time-surface) the smaller their differential time-delays.

Most of the above theorems require that we be able to distinguish the image type (L, H, or S), for which the pre-requisite is that parities should be measured. Presently, VLBI seems to be the only way to obtain parity information. It has been already used in 0957+561 (Porcas *et al.* 1981, Gorenstein *et al.* 1984), and there are good prospects in 2016+112. For the rest of the lenses, the only hope is that the Hubble Space Telescope may be able to resolve the fuzz around the lensed quasar images. If there is any asymmetry in the fuzz, then this could be used to infer image pari-ties.

REFERENCES

Blandford, R., Narayan,R., and Nityananda, R. 1986, *Ap. J.*, in press.

Bourassa, R. R., and Kantowski, R. 1975, *Ap. J.*, 195, 13.

Burke, W. L. 1981, *Ap. J. (Letters)*, 244, L1.

Florentin-Nielsen, R. 1984, *A. & A.*, 138, L19.

Gorenstein, M. V. *et al.* 1984, *Ap. J.*, 287, 538.

Gott, J. R. 1984, *Ap. J.*, 288, 422.

Greenfield, P. E. 1981, Ph. D. Thesis, M.I.T.

Hogan, C. J., and Narayan, R. 1984, *M.N.R.A.S.*, 211, 575.

Narasimha, D., Subramanian, K., and Chitre, S. M. 1982, *M.N.R.A.S.*, 200, 941.

Narasimha, D., Subramanian, K., and Chitre, S. M. 1984, *M.N.R.A.S.*, 210, 79.

Nityananda, R. 1986, preprint.

Porcas, R. W. *et al.* 1981, *Nature*, 289, 758.

Poston, T., and Stewart, I. N. 1978, *Catastrophe Theory and its Applications* (London:Pitman).

Sanders, R. H., van Albada, T. S., and Oosterloo, T. A. 1984, *Ap. J. (Letters)*, 278, L91.

Schneider, P. 1985, *A. & A.*, 143, 413.

Schneider, D. P. *et al.* 1986, preprint.

Subramanian, K., and Chitre, S. M. 1984, *Ap. J.*, 276, 440.

Vilenkin, A. 1984, *Ap. J. (Letters)*, 282, L51.

Young, P. *et al.* 1980, *Ap. J.*, 241, 507.

Young, P. *et al.* 1981a, *Ap. J.*, 244, 723.

Young, P. *et al.* 1981b, *Ap. J.*, 244, 736.

DISCUSSION


**Subramanian** : (1). Fermat's principle is a very nice way of looking at lensing by a mass sheet at a particular redshift but when you have lenses at different redshifts, then Fermat's principle formalism becomes less intuitive and useful.

(2).To add to your list of general theorems on lensing : Stephen Cowling and I have proved a number of theorems on local conditions on the surface density of the lens for multiple imaging by smooth and bounded gravitational lenses. (MNRAS in Press)

**Narayan** : (1).If the image splitting is produced by only one lens sheet and the others at different redshifts merely modify the images without introducing extra splitting, then some of the single lens-plane ideas can be carried through (BNN). However, if there is strong lensing in more than one plane,the geometrical intuition provided by Fermat's principle seems to be lost (though the principle of extremum time is still valid).

**Rees** : (1). Even those who advocate cosmic strings as triggers for galaxy formation would only expect them to contribute $10^{-5}$-$10^{-4}$ of the critical cosmological density. The probability of observing lensing due to a string, along a given line of sight, would be only of this order, so doesn't this make it unlikely that strings are relevant to observed lensing ?

(2). Could you comment on how "minilensing" might affect your discussion of the number and relative brightness of the multiple images?

**Narayan** : (1). This is substantially correct. However, if the luminosity functions of quasars were sufficiently steep [ $\phi(>L) \propto L^{-\alpha}$ ; $\alpha > 2$] then the probability of lensing by a particular class of lens could be significantly greater than the $\Omega$ in those lenses because of 'amplification bias'. The effect is absent for a straight string since it produces no magnification, but could be important for string loops (see Hogan and Narayan 1984).

(2). Most of my discussion assumed a smooth lens potential. If there ae 'mini-lenses' present, e.g. stars, then there are two possibilities :

(a) If the angular size of the source is greater than the mean angular separation of mini-lenses, the smooth potential approximation is valid.

(b) If not, each image is split into a large number of mini-images which cannot in general be resolved. The net magnification of an image can be substantially modified, and this has been invoked to explain the absence of the odd image in several observed examples of lensing. Time-delays are not affected.